Vision system for optical quality control of components made by fibre thermoplastic-based composites

Giulio D'Emilia
University of L'Aquila
Department of Industrial and Information Engineering and of Economics
L'Aquila, Italy
giulio.demilia@univaq.it

Antoniomaria Di Ilio
University of L'Aquila
Department of Industrial and Information Engineering and of Economics
L'Aquila, Italy
antoniomaria.diilio@univaq.it

Antonella Gaspari
Polytechnic of Bari
Department of Mechanics, Mathematics and Management
Bari, Italy
antonella.gaspari@poliba.it

Emanuela Natale
University of L'Aquila
Department of Industrial and Information Engineering and of Economics
L'Aquila, Italy
emanuela.natale@univaq.it

Antonios G. Stamopoulos
University of L'Aquila
Department of Industrial and Information Engineering and of Economics
L'Aquila, Italy
antonios.stamopoulos@univaq.it

Luciano Chiominto
University of L'Aquila
Department of Industrial and Information Engineering and of Economics
L'Aquila, Italy
luciano.chiominto@student.univaq.it

2021 IEEE International Workshop on Metrology for Industry 4.0 & IoT (MetroInd4.0&IoT) | 978-1-6654-1980-2/21/$31.00 ©2021 IEEE | DOI: 10.1109/METROIND4.0IOT51437.2021.9488458

***Abstract*— In this paper a contribution to the set-up and optimization of the fabrication process of thermoplastic-based composites is made. Measurements are carried out of some parameters of interests, related to the regularity of texture. Some measuring techniques are used, all based on a vision system, but different with reference to the processing algorithms of the obtained images. Image processing methods based on artificial intelligence are also used. The analysis can allow to optimize the experimental set-up and the procedure in order to obtain a suitable level of uncertainty for an effective control of the production process.**

Keywords—thermoforming, composite materials, quality assessment, vision system, uncertainty

I. INTRODUCTION

Nowadays, the thermoplastic composite materials, reinforced either with short or with continuous fibre reinforcement, are gaining the interest of many industrial applications due to their advantages compared to the thermoset based ones, especially due to their recyclability and their mass production capacity [1].

Of great interest are both the structural, mechanical and the aesthetical characteristics of the produced thermoplastic composite parts. Especially the first ones, are strongly related to the constituents of the composite material. Thus, defects introduced either to the fibre fabric or the matrix may degrade the mechanical properties related to them. For instance, the fibre misalignment is a dominant defect of the tensile and compressive properties of these materials [2]. This fibre misalignment is the result of the decrease of the capability of the matrix to maintain the position of each strand. On the other hand, this phenomenon is the basis of the drapability and deformability of these materials while they are thermoformed. To this end, several mechanisms like fibre shearing and bending of the textile are deforming the proper 0-90° positioning of the fabric as seen in [3-5]. These phenomena are usually being addressed experimentally by performing large deformation mechanical tests such as the bias-extension and the rotational bending which are complicated and conducted in the temperatures of reference in which each material can be thermoformed. Usually, the output of these tests is the basis of a process simulation using Finite Element (FE) modelling as indicated in [6-8].

The process simulation strategy plays a fundamental role as for the process optimization, even though many aspects should be taken into account, with reference to both physical and chemical characteristics of materials and real operating condition during the production phase [9-14], but integration with experimental activity is an unavoidable aspect of the approaches aiming at the optimization of the production process.

Furthermore, among the existing standardized mechanical tests that are able to evaluate their mechanical characteristics (shear, bending, fracture toughness), even full scale tests, are complex and difficult to implement, taking into account the whole range of operating temperatures and applications [1]. In some cases, very specific methods have been used for validating the simulation results, like in [9-10], where FE simulation results are assessed using X-ray, computed micro-tomography (μCT) and optical microscopy, which are not easy to implement for in-line process control.

In many cases useful information is derived also from more simple optical measurements, which can be of different types, laser systems or vision ones, aiming at identifying the fibre orientation and geometry, defect localization, surface roughness [11,12]; in [11] the real fibre architecture of preforms is captured by the optical measurement system, which generates a three-dimensional model containing information about the fibre orientation along the entire surface of the preform. In [12] many laser-based sensors can be used simultaneously to get a complete picture of the texture on the surface, suitable for assessing the simulation suggestions with reference to the production process. The use of these technologies allows the punctual identification of local defects that influence the full scale mechanical performance of the produced part.

The measurement and inspection techniques, in the most modern industrial contexts, are often integrated with artificial intelligence tools [16]. In particular, an increasing number of applications are based on the semantic segmentation of images. Flaws detection is a special case of semantic segmentation, which presents specific critical issues, due to the highly irregular shapes of defects, in the most cases. This difficulty is even greater in the case of varying textures and patterns in the image background [17-22], as in the case of composite materials.

Nevertheless, the capability of identifying undesired imperfections and defects by experimental, validated techniques also in non-favorable conditions could be a great support for process optimization, especially when simulation is difficult to apply. To get reliable results, critical analysis of the experimental apparatus and of the used data processing techniques is requested.

In order to achieve this scope, in section II the experimental set-up and the image processing techniques will be described to identify texture defects on a surface of a fibre composite material. Description of techniques aim also at highlighting the most critical aspects of each technique.

Section III presents the results of the above methodology when flat plates are analyzed and parts with surface defects. Pros and cons of each approach are also discussed, based also on a detailed statistical analysis of results.

Conclusions and future work description end the paper.

II. Materials and Methods

In the present work, a thermoplastic composite material is considered, consisting of a polypropylene matrix reinforced with a woven 2-2 twill E-glass textile by roughly 47%. This value represents the volumetric percentage of fibre, and therefore not directly comparable with the percentage value referring to the area of fibre, visible on the surface of the composite, studied in this work, but it is certainly related to it.

For the inspection of the surface, a vision system is proposed, described in the scheme of Fig.1, based on a FLIR Polarized Camera, Sony IMX250MZR sensor, 2448x2048 pixels.

Different processing techniques are compared, including a semantic segmentation algorithm, to identify a specific characteristic of a fibre thermoplastic-based composite. The characteristic of interest is the percentage of the total area occupied by the fibre, which is a parameter of interest, because its variations can be representative of fibre misalignment and anomalies present on the texture of the material.

Images of a flat composite panel without defects will be analyzed and, furthermore, images containing a specific defect (called “burn” in the following), will also be examined and compared with the former. This defect, even though is considered mostly an aesthetical flaw, is associated also with the absence of polymer on the top of the fibre tows due to excessive conditions of heating and/or local adhesion between the composite material and the pressing tools in case they are produced using compressive moulding.

This type of defect is not easily predictable by simulation, so a quick and simple method of inspection is required for the prompt identification of the presence of the defect, and the possible correction of the process parameters.

A program of experimental trials has been designed, in order to highlight the main contributions to the variability of measurements, referred to lighting and distance of camera, and algorithms set up.

The “Glare Reduction” option, offered by the polarized camera, has been used to improve image quality.

For each light direction, only the darkest pixels from each polarization quadrant are selected to reduce the influence of glares. Consequently, the image height and width are half the size of the source image. For this reason, all the pictures have 1224 x 1024 pixels dimension. For each image, in addition to the grayscale, the radiance heat-map is also acquired. This is automatically generated by the acquisition software.

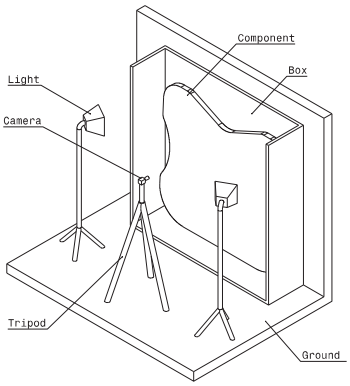

Fig. 1. Scheme of the vision system.

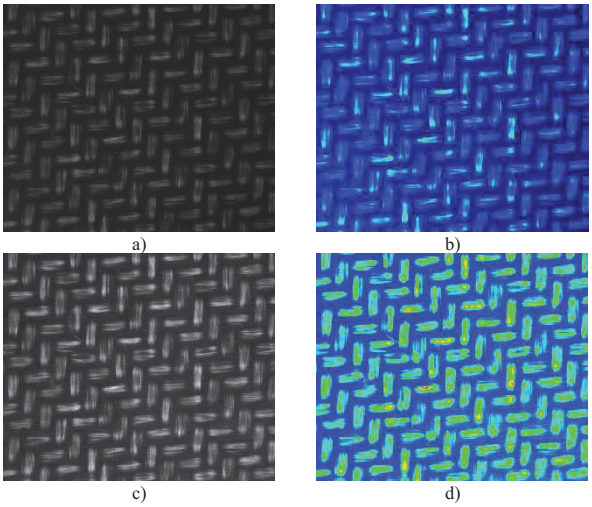

Fig. 2. a. Image with glare reduction using 1 light; b. Heat-map image using 1 light; c. Image with glare reduction using 2 lights; d. Heat-map using 2 lights.

As far illumination, two soft-boxes with 80W lamp bulbs are used (Fig. 1).

On the glass fibre reinforced polypropylene plate, 24 areas without any defects are identified and taken as reference. Consecutively, images have been acquired from three distances of camera: 150 mm, 200 mm and 250 mm.

Moreover, two different illumination conditions, the first using only one light (*ill 1*), the other using both of them (*ill 2*), have been realized. In total, 144 images (24 areas x 3 distances x 2 lighting conditions) are acquired on areas without defects.

Using the same conditions of lighting and distances, 144 pictures of defected areas (burned areas) are acquired. The "burn" defect appears as a localized enlargement of the area with fibre, and a consequent matrix extent reduction (Fig. 3).

Regarding resolution, with a distance of 150 mm the framed area is 57 x 47 mm, where each pixel has a dimension of 47 µm. At 200 mm, the framed area is 72 x 60 mm and each pixel measures 59 µm. At a distance of 250 mm between the camera and the plate, the framed area is 90 x 75 mm and each pixel is 73 µm in size.

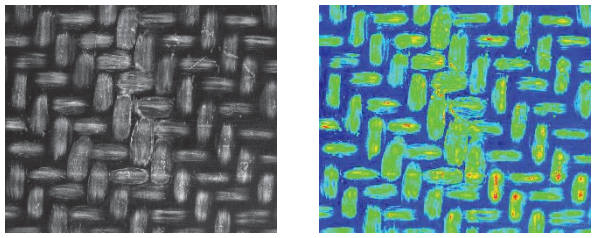

Fig. 3. a. Greyscale image of a "burn" defect; b. heat-map of a "burn" defect.

The image processing methods considered in this work are:

A. Edge detection
B. Color Indexing
C. K-Means
D. Deep Learning

All the proposed methods are developed in Matlab, and are based on the creation of a black and white mask where the white pixels correspond to the fibre, while the black ones to the matrix. Therefore, the ratios of fibres to the total area, are calculated as ratios between pixels.

A. Edge detection

Starting from a grayscale image, the output of an edge detection algorithm is a black and white image where the white pixels correspond to a detected edge. In this case, the "Canny" method is used as detection algorithm [23]. The "Canny" algorithm differs from the other edge-detection methods in that it uses two different thresholds (to detect strong and weak edges), and includes the weak edges in the output only if they are connected to strong edges. This method is therefore less likely than the others to be affected by noise, and more likely to detect true weak edges.

Regarding the high and low thresholds, these are not specified, but they are automatically calculated by the Edge function implemented in Matlab.

The edge lines in the binary mask do not delineate quite well the outline of the object of interest, because of gaps.

For this reason, a horizontal and a vertical structuring element of 6 pixels are created and the binary mask is dilated using these structuring elements.

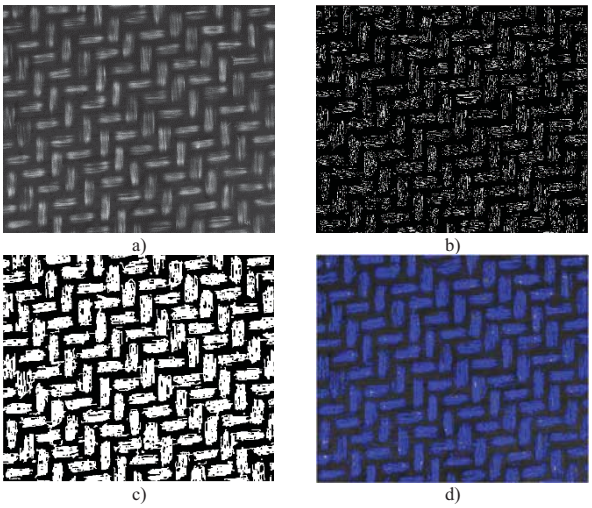

Fig. 4. a. Grayscale image; b. Detected edges; c. Mask after dilatation and erosion; d. Mask over original image.

To enhance and smooth the borders of the binary mask, the objects are eroded using a diamond shaped structuring element of 1-pixel size. The ratios of the surface fibre and matrix are calculated from the binary mask (Fig. 4).

B. Color Indexing

Considering the radiance heat-map, the colors are reduced and indexed in order to select each of them individually [24]. In this case, the number of colors has been chosen equal to 3, to take into account the different shades of the fibres. In fact, in some areas, the matrix is thicker and the fibres reflect less light, then in the heat-map they appear darker than the totally visible fibres; in any case, both classes are considered as fibre areas. Selecting the corresponding colors of the fibre areas, a binary mask is obtained and the percentage of white and black pixels are calculated (Fig. 5).

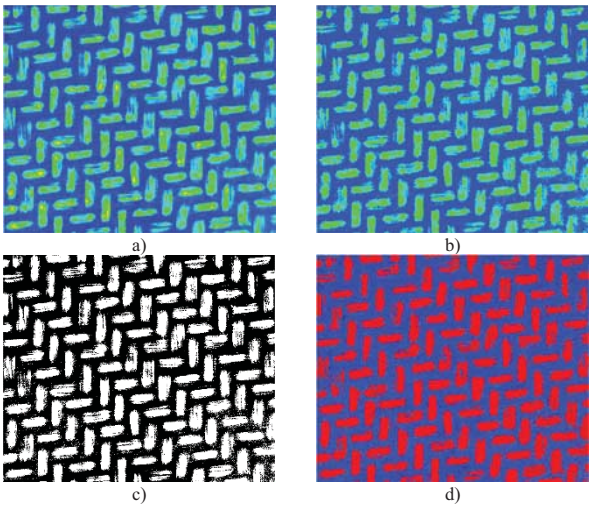

Fig. 5. a. Original image; b. Color indexed image; c. Binary mask; d. Mask over original image.

C. K-means

Considering the radiance heat-map, to group pixel by color, the color space of the image is converted from RGB

to L*a*b [25]. The L*a*b* space consists of a luminosity layer "L*", chromaticity-layer "a*" indicating where color falls along the red-green axis, and chromaticity-layer "b*", indicating where the color falls along the blue-yellow axis. To cluster the pixel by color, the K-means algorithm is used [25]. In this case, the algorithm groups in three clusters because the fibres present different shades where overlay matrix is thicker, as said. Selecting the two groups of pixels that represent the fibres it is possible to generate a binary mask where white pixels denote fibres, while black ones indicate matrix (Fig. 6). The percentage of fibre is calculated as the ratio of white pixels on the binary mask.

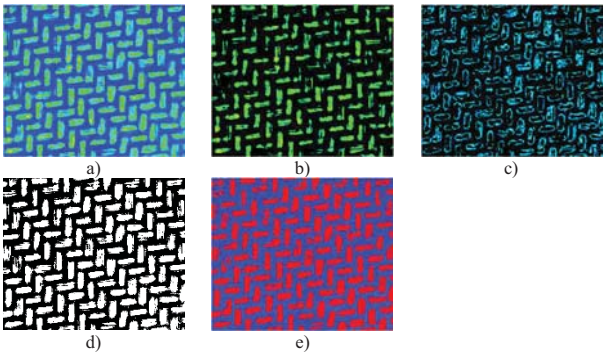

Fig. 6. a. Original image; b. and c. Clustered fibres; d. Binary mask; e. Mask over original image.

D. Deep Learning

The radiance heat-map is analyzed using a semantic segmentation neural network. In this case, DeepLabV3+ algorithm is used and it is built using ResNet18 as a feature extraction network. The network segments the fibres and the matrix on the image. The output of the semantic segmentation is a matrix of the same dimension of the image, where every element is the label of the corresponding pixel in the picture. From this matrix a binary mask is generated, where pixels labelled as "Fibre" are associated with the value 1, otherwise 0, and the percentage of white pixels is calculated (Fig. 7).

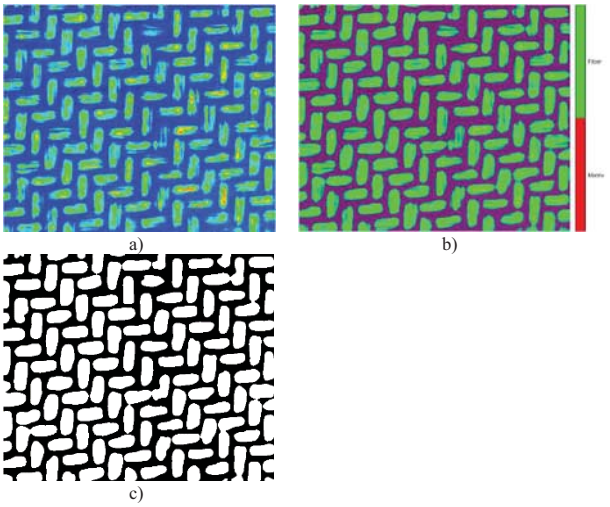

Fig. 7. a. Original Image; b. Segmented Image; c. Binary mask.

The net is trained using 24 pictures, in the described conditions of lighting and camera distances. These images are labelled in two categories: "Fibre" for the pixels that represent the visible fibreglass on the surface, and "Matrix" for the matrix elements.

The dataset is partitioned as

- 14 images for training
- 8 images for testing
- 2 images for validation

To reduce the possibility of overfitting, a data augmentation has been carried out, which involves random reflections in the left-right and top-bottom direction, rotations in the range [-45 °, 45 °], and translations in the range of 10 pixels along x- and y-axes.

The network is trained for 140 Epochs, using the stochastic gradient descent with momentum (SGDM) optimizer [26], with a momentum of 0.9, initial learning rate of 0.01, reduced by the 20% every 10 epochs.

III. RESULTS

The results of the image analysis are summarized in Figs. 8-11, where the percentage of fibre calculated in images without defects, acquired in different conditions of lighting (*ill 1* and *ill 2*) and camera distance (150 mm, 200 mm, 250 mm), are shown, with reference to each processing method. The variability, in terms of standard deviation, is represented as error bars.

Each graph also indicates the percentage of pixels that represents the fibre extent in the case of an image with defect. Only an image with "burn" is considered in these graphs, because the variability calculated on different images, would be indicative of the different extension of the defective areas, and not of the variability of the method in determining the percentage of fibre.

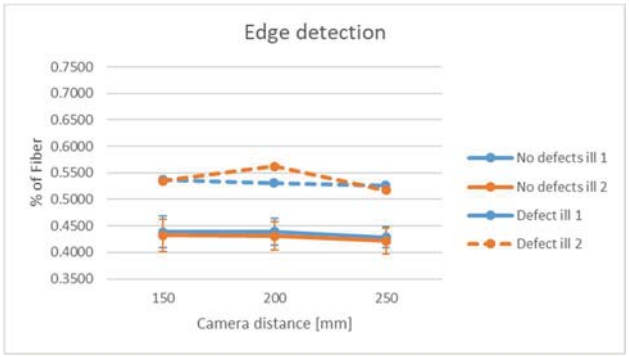

Fig. 8. Fibre percentage, as calculated by the edge detection method.

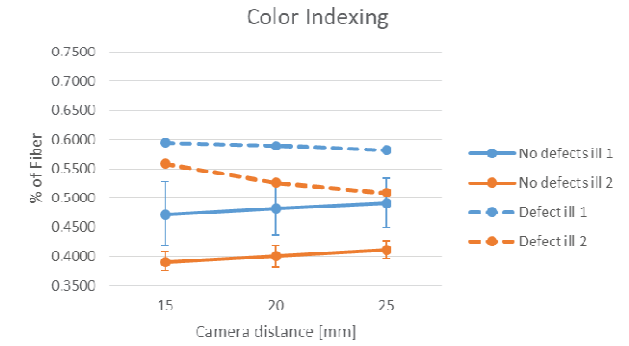

Fig. 9. Fibre percentage, as calculated by the color indexing method.

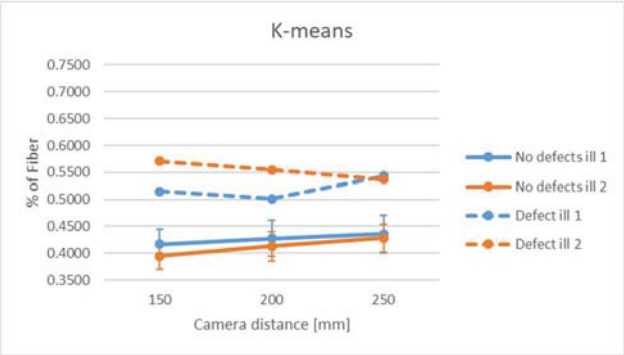

Fig. 10. Fibre percentage, as calculated by the K-means method.

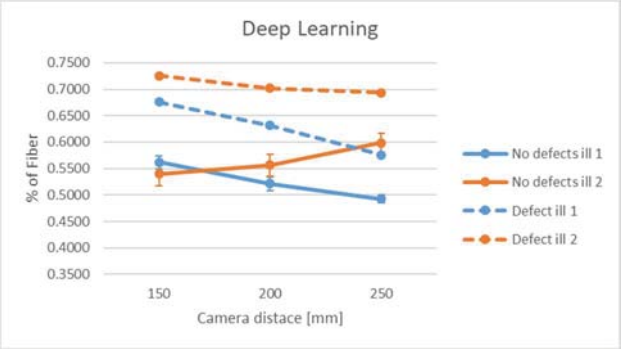

Fig. 11. Fibre percentage, as calculated by the deep learning method.

With reference to the semantic segmentation method, the performance of the network in the training phase can be measured by the average of the *Intersection over union (IoU)* or *Jaccard index* [27], which, in the training phase, results to be equal to 0.82, that is a satisfactory value.

Figures show that in all cases the percentage of fibre, in case of absence of defects, is in the range 0.4 ÷ 0.6; these are plausible values, given that the volumetric percentage of the fibres is 47%.

In particular, Fig. 8 and Fig. 10 show that there are no significant variations in the percentage value, by changing lighting or camera distance, when the Edge detection or K-means methods are used.

Instead, Fig. 9 and Fig. 11 show that illumination conditions can significantly affect the results, in Color indexing and Deep learning methods; in deep learning, the camera distance can also produce significant variations in results. Also taking into account the long labeling and training times, the semantic segmentation method appears not preferable in this application.

On the contrary, Edge detection is particularly advantageous, both from the point of view of the simplicity of implementation, and of the insensitivity to the influence parameters.

For all methods, it is found an increase over the 15% in the fibre percentage when an image with burns, as that in Fig. 3, is analyzed. This trend is present in all the considered conditions. Hence, this result suggests the possibility of using one or more of these approaches to detect the presence of this type of defect.

IV. CONCLUSIONS AND FUTURE WORK

With reference to a glass fibre thermoplastic-based composite, in this paper a polarized camera for the acquisition of images has been used, and different processing techniques have been compared, to identify the percentage of the total area occupied by the fibres. This value represents a surface characteristic of interest, because its variations can be representative of anomalies present on the texture of the material.

Images of a flat plate without defects, and images containing the “burn” defect, have been examined and compared, by using different image processing methods, including semantic segmentation.

An analysis of the main aspects affecting the accuracy of methods has been carried out, in particular lighting and distance of measurement.

The results show that some methods are less sensitive to the variation of the influence parameters, and also less onerous from an operational point of view. In addition, they appear promising from the point of view of the identification of superficial defects, like “burns”.

REFERENCES

[1] Di Ilio A., Di Genova L.G., Stamopoulos A.G., Implementation of the modified V-Notched Rail Shear method for characterizing glass fiber thermoplastic composites at sub-zero and elevated temperatures, Polymer Testing, (2021), 93, 106174

[2] Zheng T., Guo L., Shun R., Li Z., Zhu H. Investigation on the compressive damage mechanisms of 3D woven composites considering stochastic fiber initial misalignment. Composites Part A: Applied Science and Manufacturing 2021. https://doi.org/10.1016/j.compositesa.2021.106295.

[3] P. Boisse, N. Hamila, E. Vidal-Sallé, F. Dumont. Simulation of wrinkling during textile composite reinforcement forming. Influence of tensile, in-plane shear and bending stiffnesses. Composites Science and Technology. 71 (2011) 683-692.

[4] Wang P.,Hamila N., Boisse P., Intraply shearing characterization of thermoplastic composite materials in thermoforming processes. Key Engineering Materials 2012; 504-506: 243–248.

[5] Lussier D., Chen J. Material characterization of woven fabrics for thermoforming of composites. Journal of Thermoplastic Composite Materials 2002; 15(6):497-509.

[6] Di Ilio A., Stamopoulos A.G. On the predictive tools for assessing the effect of manufacturing defects on the mechanical properties of composite materials. Procedia CIRP 2019; 79: 563-567.

[7] Stamopoulos A., Di Ilio A. Numerical and experimental analysis of the thermoforming process parameters of semi-spherical glass fiber thermoplastic parts. Procedia CIRP, Proceedings of the 14th CIRP Conference on Intelligent Computation in Manufacturing Engineering, CIRP-ICME ‘20, Italy.

[8] Haanappel S.P., Ten Thije R.J.W., Sachs U., Rietman B., Akkerman R. Formability analyses of uni-directional and textile reinforced thermoplastics.

[9] Zhang H., Chen J., Yang D., Fiber misalignment and breakage in 3D printing of continuous carbon fiber reinforced thermoplastic composites, Additive Manufacturing, Volume 38, February 2021, Article number 10177.

[10] Tserpes K.I., Stamopoulos A.G., Pantelakis S.G. A numerical methodology for simulating the mechanical behavior of CFRP laminates containing pores using X-Ray computed tomography data. Composites Part B: Engineering (2016), 102, pp.122-133.

[11] Duboust N., Watson M., Marshall M., O’Donnel G.E., Kerrigan K., Towards intelligent CFRP composite machining: surface analysis methods and statistical data analysis of machined fiber laminate

surfaces, Proceedings of the Institution of Mechanical Engineers, Part B: Journal of Engineering Manufacture (2020), article in press.

[12] Semlali Aouragh Hassani, F.Z., Achaby M.E., Bensalah M.O., Rodrigue D., Boufidh R., Qaiss A.E.K.,Injection molding of short fiber thermoplastic bio-composites: Prediction of the fiber orientation, Journal of Composite Materials Volume 54, Issue 30, 1 December 2020, Pages 4787-4797

[13] Stamopoulos, A.G., Spitilli, P., D'Emilia, G., Gaspari A., Natale, E., Di Ilio, A., Assessment of the measurements contribution on composites thermoforming processes: A case study of an automotive component, 2020 IEEE International Workshop on Metrology for Industry 4.0 and IoT, MetroInd 4.0 and IoT 2020 - Proceedings, 2020, pp. 299–303, 9138197.

[14] D'Emilia, G., Di Ilio, A., Gaspari, A., Natale E., Perilli, R., Stamopoulos, A.G., The role of measurement and simulation in additive manufacturing within the frame of Industry 4.0, 2019 IEEE International Workshop on Metrology for Industry 4.0 and IoT, MetroInd 4.0 and IoT 2019 - Proceedings, 2019, pp. 382–387, 8792876.

[15] D'Emilia G., Di Ilio A., Gaspari A., Natale E., Stamopoulos A. G., Uncertainty assessment for measurement and simulation in selective laser melting: a case study of an aerospace part, ACTA IMEKO, Vol. 9 (4), 2020, 96-105.

[16] [pp] Alonso, V., Daca-Nieto, A., Barreto, L., Amaral, A., Rivero, E.: Industry 4.0 implications in machine vision metrology: an overview, 8th Manufacturing Engineering Society International Conference, Procedia Manufacturing, Vol. 41, 2019, pp. 359–366.

[17] [a] Das, S., Hollander, C. D., & Suliman, S. (2019, September). Automating Visual Inspection with Convolutional Neural Networks. In Annual Conference of the PHM Society (Vol. 11, No. 1).

[18] [f] Tabernik, D.; Šela, S.; Skvarc, J.; Skocaj, D.: Segmentation-based deep-learning approach for surface defect detection, Journal of Intelligent Manufacturing, Vol. 31., 2020, pp. 759–776.

[19] [g] Racki D., Tomazevic, D., Skocaj D.: A compact convolutional neural network for textured surface anomaly

[20] detection, IEEE Winter Conference on Applications of Computer Vision, Lake Tahoe, NV, United States ,March 12-15, 2018.

[21] [h] Qian K.: Automated detection of steel defects via machine learning based on real-time semantic segmentation, ACM International Conference

[22] Liu, Y., Yang, Y., Wang, C., Xu, X., Zhang, T.: Research on Surface Defect Detection Based on Semantic Segmentation, 2019 International Conference on Artificial Intelligence, Control and Automation Engineering (AICAE 2019), 2019, pp. 403-407.

[23] https://it.mathworks.com/help/images/ref/edge.html

[24] https://it.mathworks.com/help/matlab/ref/rgb2ind.html

[25] https://it.mathworks.com/help/images/color-based-segmentation-using-k-means-clustering.html

[26] https://it.mathworks.com/help/deeplearning/ref/trainingoptions.html

[27] Fernandez-Moral, E., Martins, R., Wolf, D., & Rives, P. (2018, June). A new metric for evaluating semantic segmentation: leveraging global and contour accuracy. In 2018 ieee intelligent vehicles symposium (iv) (pp. 1051-1056). IEEE.